Evolution of fragment-fragment correlations in reactions of ^{197}Au and ^{107,109}Ag with ^{40}Ar from 7 A to 34 A MeV

T. Ethvignot,[1,2] N. N. Ajitanand,[1] J. M. Alexander,[1] E. Bauge,[1,2] A. Elmaani,[1] L. Kowalski,[1] M. Lopez,[1] M. T. Magda,[1] P. Désesquelles,[2] H. Elhage,[2] A. Giorni,[2] D. Heuer,[2] S. Kox,[2] A. Lleres,[2] F. Merchez,[2] C. Morand,[2] D. Rebreyend,[2] P. Stassi,[2] J. B. Viano,[2] F. Benrachi,[3] B. Chambon,[3] B. Cheynis,[3] D. Drain,[3] and C. Pastor[3]

[1]*State University of New York at Stony Brook, Stony Brook, New York 11794*

[2]*Institut des Sciences Nucléaires de Grenoble, Institut National de Physique Nucléaire et de Physique des Particules–Centre National de la Recherche Scientifique/ Université Joseph Fourier, 53, Avenue des Martyrs, 38026, Grenoble CEDEX, France*

[3]*Institut de Physique Nucléaire de Lyon, Institut National de Physique Nucléaire et de Physique des Particules–Centre National de la Recherche Scientifique/Université Claude Bernard, 43, Boulevard du 11 Novembre 1918, Villeurbanne CEDEX, France*

(Received 27 March 1992)

In-plane and out-of-plane angular correlations have been measured between fragments of $Z>3$, Li fragments, ^{3,4}He, and ^{1,2,3}H. The changing patterns for ^{40}Ar induced reactions of 7 A, 17 A, 27 A, and 34 A MeV give an overview of the decreasing importance of mass-symmetric fissionlike reactions at the expense of a broad range of more mass-asymmetric breakups. Evidence is given that these fragments come from a central collision group of reactions that have similar violence and from which many combinations of fragments and particles are ejected. Very similar azimuthal angular correlations are observed for particles with a Li fragment and for particles with a pair of heavier fragments ($Z>3$). This similarity suggests comparable strengths of association with the reaction plane for single Li fragments and for fragment pairs of $Z>3$. Azimuthal angular correlations for Li-Li pairs exhibit distinct asymmetries; their interpretation via trajectory-model calculations indicates mean delay times of $\approx 5\times 10^{-22}$ s.

PACS number(s): 25.70.Pq

I. INTRODUCTION

For many years the angular correlations between fission-fragment pairs have served as an experimental probe of linear momentum transfer in nuclear reactions [1]. In addition, the angular distributions of single fission fragments, α particles, etc., have been extensively studied in relation to angular momentum deposition into composite nuclei and its effect on their decision-point shapes, temperatures, decay modes, etc. (see, for example, Refs. [2–5] and references therein). Recent correlation studies have emphasized intermediate-energy [$\approx$(10–100) A MeV] heavy-ion reactions (see Refs. [1–12] and references therein) and have sought information on the reaction dynamics as well as on the hot nuclei produced.

During the first years of availability of heavy-ion beams of $>15\,A$ MeV, many such studies were made that involved fragment-fragment coincidence measurements with relatively small detectors. The results for the average linear momentum transfer (LMT) follow a rather clear systematic pattern, but there is confusion about the yields for the various reaction classes (i.e., high LMT versus low LMT) [6–12]. Since these studies generally involved experimental setups with limited out-of-plane angle acceptance, it was not possible to get good azimuthal angular integrations of the coincidence cross sections. With the capabilities of a 4π multidetector [13–16] it is possible to work toward an overview of the coincidence patterns for both in-plane and out-of-plane angular correlations.

This paper is one of a series [17–19] in which charged particles and fragments registered in the AMPHORA multidetector [13] have been used to survey the evolution of ^{40}Ar reactions from low to intermediate energies, i.e., 7 A to 34 A MeV. The objective here is to get a better feeling for the declining role of fissionlike fragments and the ascending role of intermediate-mass fragments. We present a survey of two-body correlations, both fragment-fragment and fragment-particle pairs. These correlations give an interesting overview of the changing character of heavy-ion reactions with increasing deposition energy.

II. EXPERIMENTAL TECHNIQUES

An experiment was performed with the AMPHORA multidetector [13] ($\approx$85% of 4π) at the Institut des Sciences Nucléaires de Grenoble. The SARA accelerator provided ^{40}Ar beams of 7 A, 17 A, 27 A, and 34 A MeV, which were used to bombard targets of Al, Cu, Ag, and Au. A typical CsI module in the multidetector was able to separate individual isotopes of H and He; also groups were identifiable for $Z=3$ (Li fragments) and for $Z>3$ (heavier fragments) [17]. Detector efficiencies (for $\theta<78°$)

were $\approx 100\%$ for essentially all detectors for H and He; efficiencies for Li and $Z > 3$ were more variable. Nevertheless, due to the great redundancy of azimuthal angle (φ) configurations, these variable efficiencies give no particular problem for the precision of observed $\Delta\varphi$ distributions. This point was tested for a number of azimuthal distributions by comparing the raw and efficiency-weighted distributions; differences were smaller than the size of the points in the figures we show below [19]. However, we estimate that there are relative errors of up to 25% for some of the points in the polar angle (θ) distributions of heavy fragments, and for H and He in singles for $\theta > 78°$. In this work we have not made corrections for these effects since they do not affect our conclusions as we show below. Most of the data reported here involves detection of Li or heavier fragments in ring 4,5,6, or 7 of AMPHORA; Fig. 1 gives a schematic diagram of the geometry. The granularity is coarse, but the angular coverage is large, which permits this geometry to give new insights compared to many earlier experiments. In particular, the azimuthal angular correlations can be examined in detail while the polar correlations are naturally rather crude.

III. RESULTS AND DISCUSSION

Azimuthal angular correlations are shown in Fig. 2 for two heavy fragments ($Z > 3$) detected anywhere in rings 4–7 ($15° < \theta < 78°$). For ^{40}Ar energies of $7A$ MeV one sees the extreme preference for in-plane ($\Delta\varphi$ near 180°) detection. This dramatizes the very familiar behavior of two-body breakup or fissionlike reactions [1]. The rather flat part of the correlation for $0° < \Delta\varphi < 150°$ signals multibody breakup reactions that have been studied in some detail for similar reactions. Boger *et al.* [20] have assigned a certain fraction of these to the ejection of an intermediate-mass fragment (IMF) followed by fission and another fraction to simultaneous ternary breakup also involving an IMF.

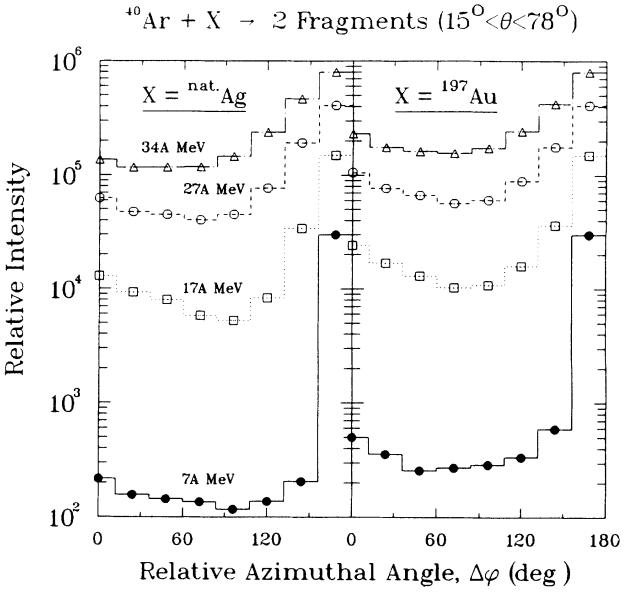

FIG. 2. Azimuthal angular correlations (θ and $\Delta\varphi$ in the laboratory frame) for fragment pairs (each $Z > 3$) for the cases indicated. Rings 4–7 were all allowed. Statistical uncertainties are shown if they extend beyond the size of the symbol.

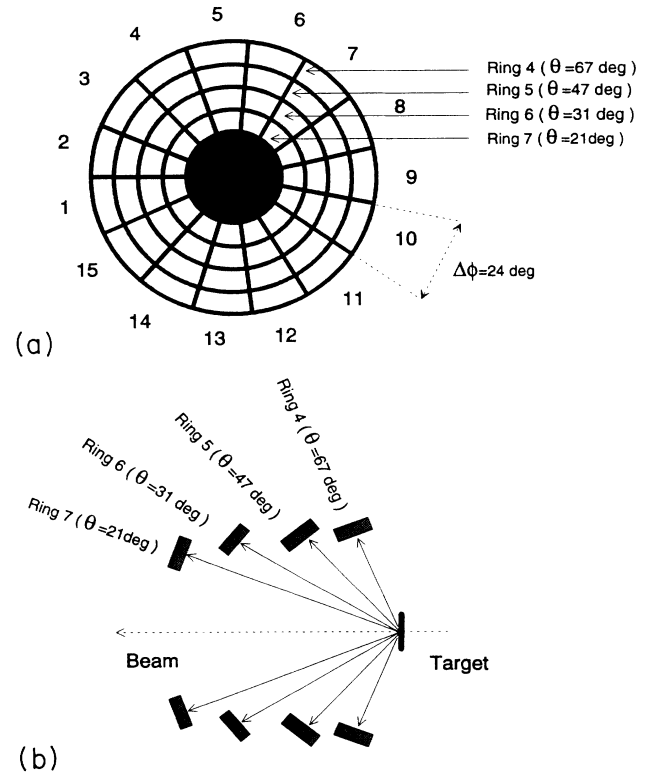

FIG. 1. Schematic diagram of the configuration of rings 4–7 of the AMPHORA multidetector (Ref. [13]). (a) View from the target in the beam direction; (b) side view.

The preference for 180° in the azimuthal correlations (Fig. 2) persists for all incident energies. However, the relative magnitude of this in-plane preference decreases as the incident energy increases. There is also a clear increase in the full width (in $\Delta\varphi$) of this in-plane peak from $< 24°$ at $7A$ MeV to $\approx 48°$ at $34A$ MeV. Figure 3 shows some of these distributions (those for both fragments detected in the same ring) for $34A$ MeV ^{40}Ar. These curves emphasize that although there is a preference for in-plane ($\Delta\varphi$ near 180°) emission, there is a quite strong intensity for out-of-plane fragment emission. For the central collision group at this high incident energy of 1356 MeV ^{40}Ar, there is evidence from other work [6,7,11,12] for thermalization of 600–700 MeV of energy and, therefore, the emission of many tens of particles. These particle chains must contribute significantly to the width of any "two-body" correlations, but we consider it likely that three or more heavy fragments are involved in these reactions where we observe a $\Delta\varphi$ value of $\leq 108°$. This third body could be a rather slow-moving heavy residue for which detection efficiency in CsI could be quite poor.

We have decomposed these $\Delta\varphi$ correlations into two components: one for $\Delta\varphi$ near 180° (often called "in-plane") and a second for all other $\Delta\varphi$ (often called "out-

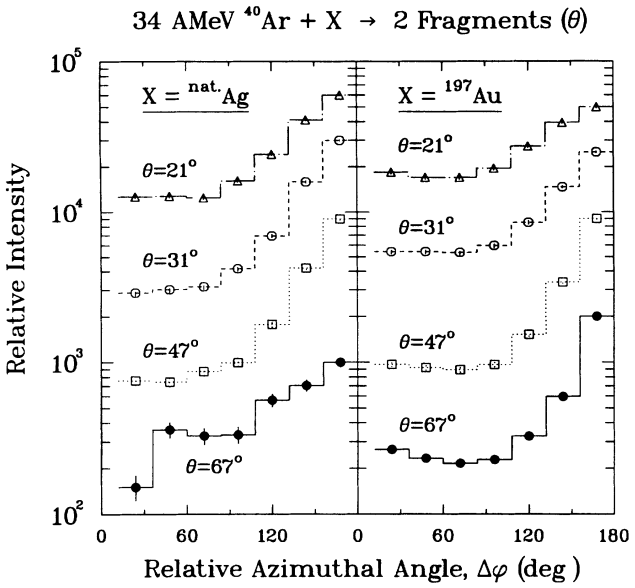

FIG. 3. Same as Fig. 2 but for two fragments ($Z > 3$) registered in the same ring.

of-plane"). This decomposition was made from plots similar to Fig. 3, but made separately for all folding-angle combinations θ_i and θ_j corresponding to each ring i and j. The method used was to average all intensity values for $\Delta\varphi < 108°$ and to define this as an appropriate "background." This background was subtracted from the intensities for $\Delta\varphi$ near 180° (i.e., $132° < \Delta\varphi < 228°$) to get an integrated intensity for $d^2\sigma/d\theta_1 d\theta_2$. Likewise, an extrapolation for this "background" was added to the intensities for the sum of all other $\Delta\varphi$ values to get a second integrated intensity for $d^2\sigma/d\theta_1 d\theta_2$.

With this procedure we have obtained the folding-angle distributions shown in Figs. 4 and 5. One should not be distracted by the somewhat jagged appearance; recall that the granularity is poor and the fragment efficiencies are somewhat variable. The important points of these figures lie in the trends. We start with the coincidence cross sections $d^2\sigma/d\theta_1 d\theta_2$ at 7A MeV and ignore, for the moment, the average multiplicities of H-He. For both Ag (Fig. 4) and Au (Fig. 5) we see a peak in the probability for in-plane folding angles near to that expected for the fusion-fission peak. Also we see that the relative abundance of "out-of-plane" fragment production is essentially negligible. In other words, the vast majority of all fragment pairs are emitted very near to a plane containing the beam axis.

Turning to the frame for 17A MeV ^{40}Ar we see marked changes in Figs. 4 and 5. As expected the fusion-fission peak in the folding angle for $\Delta\varphi$ near 180° has moved to smaller folding angles, corresponding to larger velocities of the fissioning nuclei. But now there is also a distinct tail in the correlation for small folding angles, i.e., $\theta_1 + \theta_2 < 80°$ for the Au target. Also there is substantial out-of-plane production of fragments (all other $\Delta\varphi$) from both Ag and Au for $\theta_1 + \theta_2 < 90°$. These trends continue as one moves to 27A MeV where the in-plane folding-angle peak for fusion fission becomes indistinct. Finally for 34A MeV the in-plane and out-of-plane fragment selections yield similar folding-angle distributions with no clear fusion-fission peak at all.

The disappearance of the fusion-fission peak has been reported before in studies of the in-plane correlations [21]. The interesting point here is the association with an increasing abundance of out-of-plane fragment-fragment pairs and the similarity in folding-angle distributions for out-of-plane and in plane pairs. In each frame of Figs. 4 and 5 we have also shown the average H-He multiplicity $\langle M_{Z=1,2} \rangle$ for each set of fragments. Although there are some small differences in the folding-angle dependence of these quantities, the main point is their similarity with folding angle and fragment class (for each target and ^{40}Ar energy). Apparently these fragments are all produced in reactions with high deposition energies [18]. As the ener-

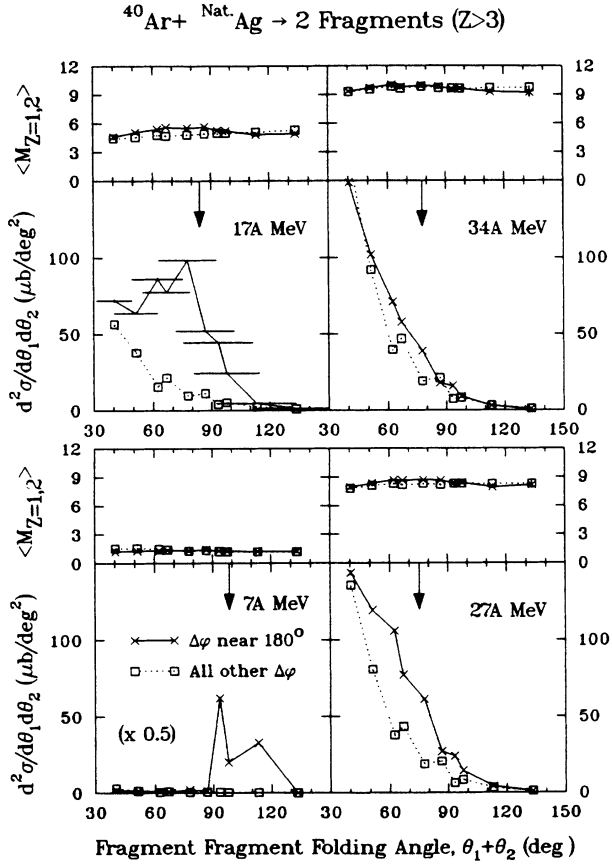

FIG. 4. Folding-angle correlations $d^2\sigma/d\theta_1 d\theta_2$ for fragment pairs (each $Z > 3$) from Ag reactions as observed in AMPHORA rings 4–7. Horizontal bars for 17A MeV give the full angular acceptance for a particle pair detected in rings i and j ($\Delta\theta_i + \Delta\theta_j$) (see Fig. 1). Fragments with "$\Delta\varphi$ near 180°" include $120° < \Delta\varphi < 260°$ (after "background" subtraction). Data for fragments with "All other $\Delta\varphi$" values are also shown. Average H-He multiplicity $\langle M_{H,He} \rangle$ as triggered by each fragment pair is shown in the upper panels. The arrows indicate the predicted folding-angle values for symmetric fission with linear momentum transfer of 100, 85, 80 , and 70% for 7A, 17A, 27A, and 34A MeV, respectively. Systematic uncertainties in the cross sections are estimated to be ±25% (see text).

gy deposited in a composite nucleus increases, it is known that the production of IMF's increases. In other words, the width of the heavy-fragment (or fission-fragment) mass-distribution curve increases. If the valley in the mass-yield curve (for $6 < A < 35$) is filled in, then there is no obvious division between fission and intermediate-mass fragment production [20], and even heavy evaporation residues (ER's) are not distinguishable from heavy residues after IMF emission [12]. The folding-angle distribution looses its peak because the folding angle is a smoothly decreasing function of the exit channel mass asymmetry [22], and all mass asymmetries are populated with comparable abundance.

More detail concerning reactions of each fragment class is given by the H-He multiplicity distributions shown in Figs. 6 and 7. Let us begin with Fig. 6(a) for $7A$ MeV ^{40}Ar+Ag. Earlier work has shown that charged particles are most often associated with ER's and that their multiplicites are much smaller in coincidence with fissionlike fragments of IMF's [23]. This is confirmed in Fig. 6(a) which shows only small H-He multiplicities in coincidence with either fragment group. In measurements to be presented later [24] we show that ER's are indeed associated with the larger H-He multiplicites.

Moving to Fig. 6(b) for $17A$ MeV ^{40}Ar+Ag, we see several interesting points. As discussed in Ref. [18] it is clear that only high-multiplicity events are selected by the trigger requirement for two H or He particles at

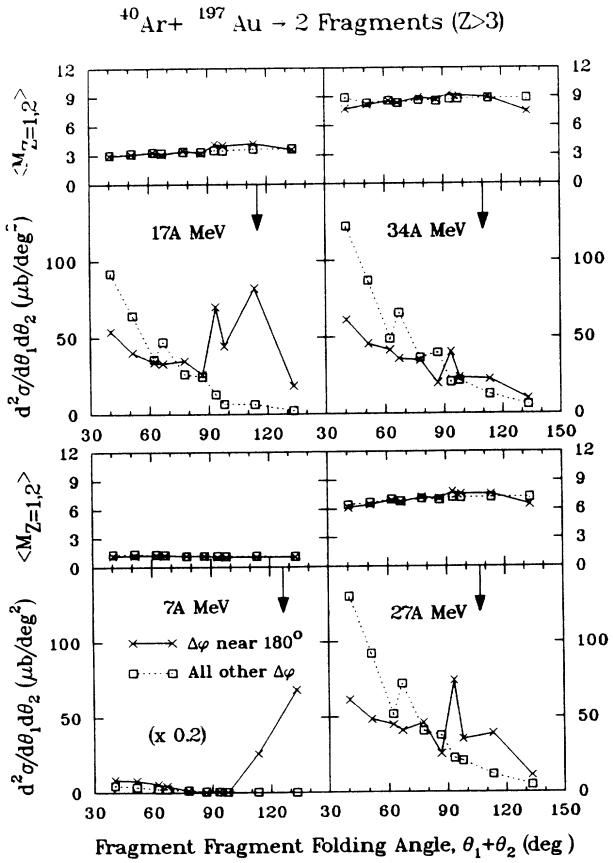

FIG. 5. Same as Fig. 4 but for Au reactions.

$\theta > 56°$. The fragment pairs, both for $\Delta\varphi$ near 180° and for $\Delta\varphi \approx 0°-150°$ (out-of-plane) have somewhat smaller average multiplicities. And finally the three-fragment events have even smaller H-He multiplicities. Results for the Au target, shown in Fig. 7(b), are very similar. Often a decrease in average multiplicity is identified with a decrease in the violence or average deposition energy. Our interpretation takes another view; it is that these triggers may well select from a central collision group with a very similar distribution in deposition energies [18]. Those nuclei that fission give products with relatively higher H-He binding energies compared to those for neutrons; thus their H-He emission is abbreviated by fission competition [23]. Finally, those reactions which emit three heavier fragments have simply evacuated more of their energy in this way and have less to spend for H-He emission.

The pattern in Figs. 6(c), 6(d), 7(c), and 7(d) shows great similarity for $27A$ and $34A$ MeV compared to $17A$ MeV. However, there are some contrasts. The two-fragment triggers seem to select a relatively narrow distribution of H-He mutiplicities that is more biased toward high violence than the trigger on two H or He particles; the latter seem to pick up a tail extending to lower multiplicities. In all cases, however, the triggers on three heavier fragments give somewhat smaller multiplicities than either of the others. Again we interpret this to indicate that these different decay channels mainly arise from a single central reaction group with essentially the same available energy content. We do not feel that it is reasonable for these latter reactions (three or more fragments) to originate from collisions of less violence than those giving two H or He or two fragments. Therefore, we feel that the H-He multiplicities do not stand alone as a gauge of relative collision violence for reactions involving multifragment production.

In the examination of the data on multiplicities in Figs. 4–7, we have been trying to expose special characteristics of those collisions that lead to certain kinds of fragments. The angular distributions of protons or α particles also provide a way to look for such special characteristics [17]. In Figs. 8 and 9 we show angular distributions of α particles triggered with some of the same fragment combinations. The first observation is that the intensity balance between forward peak and near isotropic plateau is essentially independent of the H-He or fragment trigger condition. Hence we conclude that these particular fragment triggers do not seem to select a set of impact processes that lead to fast nuclear explosions as might be anticipated for multifragmentation.

For the reactions with Ag, we see in Fig. 8 that back-angle peaking (generally associated with a spin-driven anisotropy) of the α particles is reduced by the fragment triggers. From the perspective of statistical evaporation, this could mean that the fissionlike reactions occur more rapidly (or earlier in the evaporative decay sequence) for the high-spin nuclei, thus leaving a preponderance of fragment-associated α particles to the emitters with lower spins. Alternatively, there could be a signficant contribution from near-scission α-particle emission, which occurs preferentially near to 90° from the fragments, and, there-

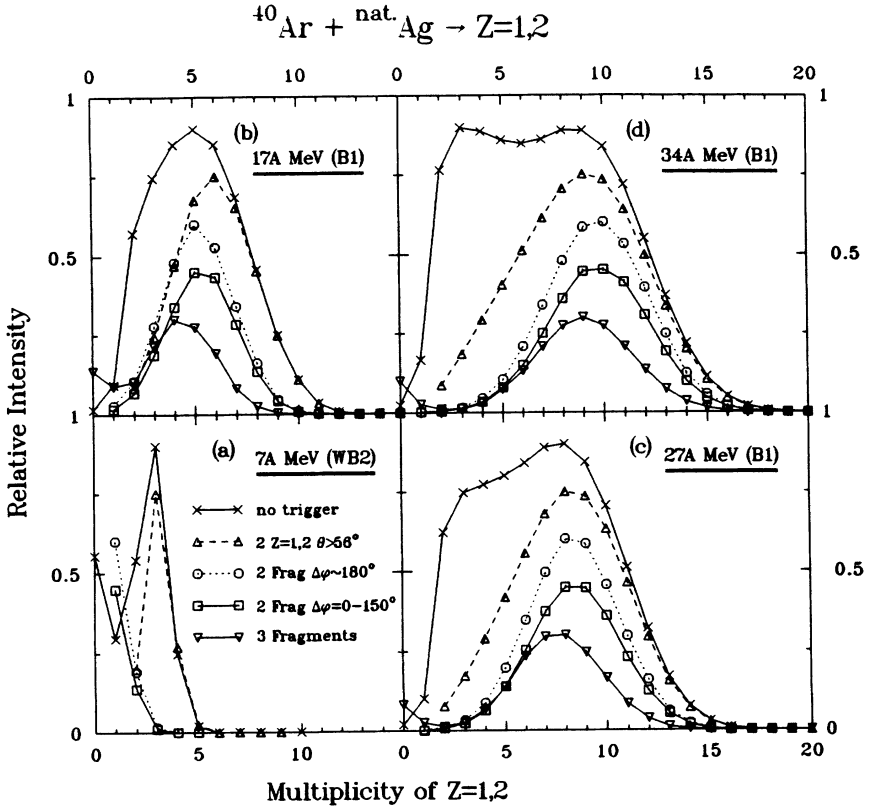

FIG. 6. H-He multiplicity distributions (arbitrary normalizations) for Ag reactions for the ^{40}Ar beam energies indicated. The separate trigger conditions are indicated. Enabling conditions are indicated in parentheses (W, AMPHORA's wall detectors; B, AMPHORA's ball detectors; digits 1 or 2 give minimum required number of detector hits for recording an event). The shapes (at low multiplicities) of the untriggered distributions are influenced by the enabling condition.

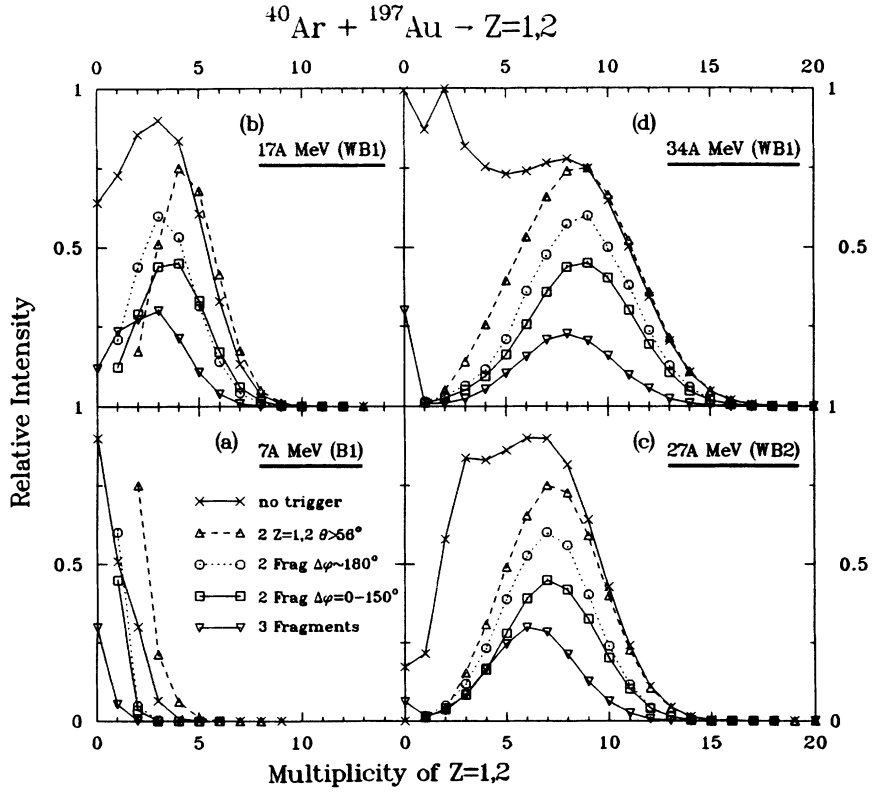

FIG 7. Same as Fig. 6 but for Au reactions.

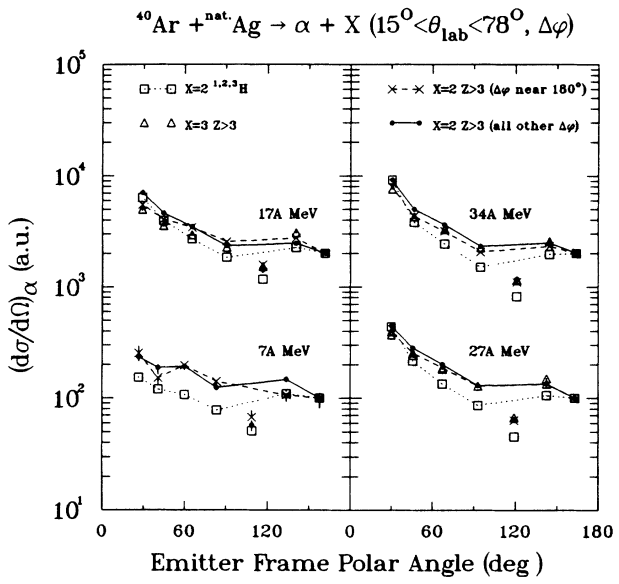

FIG. 8. Polar angular distributions in the emitter frame for α particles from Ag reactions. The emitter frame velocity was taken from measurements or systematics of the fractional linear momentum transfer (100, 85, 80, and 70% for for $7A$, $17A$, $27A$, and $34A$ MeV, respectively). The trigger conditions are indicated.

fore, with less abundance near to the 180° laboratory angle [20]. The main result, however, is the generally similar form of these angular distributions.

Let us now consolidate the information on fragment production taken from Figs. 4–9. First we see in Figs. 4 and 5 a decreasing importance of the classical fusion-fission peak as the ^{40}Ar energy is increased from $7A$ to $34A$ MeV. Apparently the fissionlike reactions have been so broadened in their mass and kinetic-energy distributions that the familiar peak in folding angle has become a smear [22]. We also see an increasing importance for

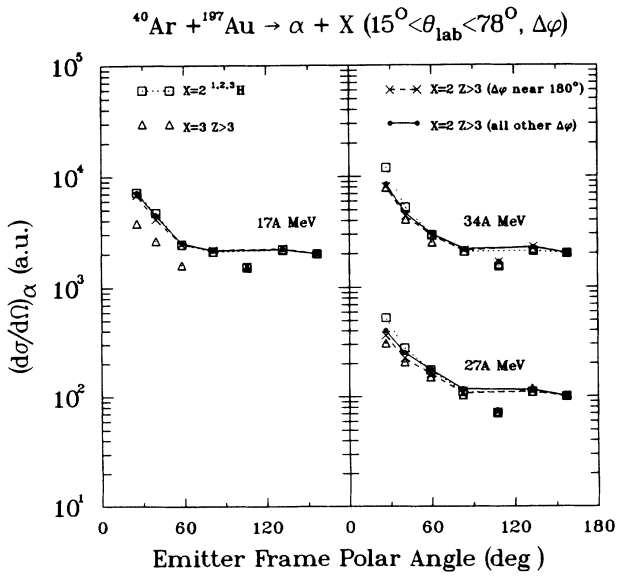

FIG 9. Same as Fig. 8 but for Au reactions.

out-of-plane fragment production (i.e., with $\Delta\varphi$ of 0°–150°) that must be associated with multibody breakups [20]. These out-of-plane fragments are not, however, associated with either unusually large H-He multiplicities (Figs. 5 and 6) or explosive forward ejection of α particles (Figs. 8 and 9). The more explicit multifragment triggers (three or more heavier fragments) also do not select especially large H-He multiplicities. In fact, these triggers generate somewhat smaller averge H-He multiplicities, probably pointing toward a fairly large central collision group of similar available energy [18].

Now we want to search for signals of a correlation between the true reaction plane (or the entrance channel spin axis normal to it) and the angles of fragment emission. A simple indicator is the strength of the azimuthal angular correlations [4,5,23,25–27]. Figure 10 shows such $\Delta\varphi$ correlations for ^{1,2,3}H, ^{3,4}He, and Li (detected in a ring at θ_2) with respect to a fragment pair detected nearly in plane in the same ring (both fragments at θ_1). (This condition corresponds to $144° < \Delta\varphi < 216°$ or to one fragment registered in detector 1 in Fig. 1 and a second fragment in detector 8 or in detector 9.) Indeed there is a clear preference for particle emission in the same plane as the fragments. These preferences generally increase with the mass of the detected particle (except for ^{3}He which is more anisotropic than ^{4}He, possibly due to its higher energy threshold), and they are almost independent of Ag or Au targets.

In Fig. 10 the anisotropies for Li fragments are quite large, indeed. One might ask whether the Li fragment itself might not be as strongly correlated with the true reaction plane as are the two heavier fragments which were the triggers. In Figs. 11 and 12 we compare $\Delta\varphi$ distributions with respect to a heavy-fragment pair and with respect to a single Li fragment. The patterns are very similar for all the anisotropies with usually a hint of slightly more strength for the trigger on fragment pairs (Fig. 11).

Another important aspect of Fig. 12 is the distinct 0°–180° asymmetry observed for Li-Li pairs, especially for the larger θ values. This point is explored in more detail in Fig. 13. Here the Li-Li azimuthal angular correlations are compared for Cu, Ag, and Au targets bombarded with $27A$ MeV ^{40}Ar. The behavior is very similar to Fig. 12 for $34A$ MeV ^{40}Ar+Ag; a preference for 180° over 0° is always observed, along with a general disfavoring for $\Delta\varphi = 90°$ (i.e., out of plane). The precision of these $\Delta\varphi$ distributions is very good, so one can pick out even rather small differences between the targets. The anisotropy or yield ratio for $(\Delta\varphi = 168°)/(\Delta\varphi = 96°)$ seems to increase very slightly from Au to Ag to Cu. Similarly the asymmetry ratio $(\Delta\varphi = 168°)/(\Delta\varphi = 0°)$ also increases from Au to Ag to Cu for both θ_1 and $\theta_2 \geq 31°$. However, the dependence on target is reversed for $\theta_1 = 21°$ and $\theta_2 = 21°$ or 31°.

For evaporationlike emission right-left emission asymmetries may be due to emitter recoil and final-state interactions [17,19,28,29]. In Fig. 14 we compare one of these data sets to several reaction simulation calculations. These calculations were made with the code COULGAN [28], which is based on nuclear evaporation theory and

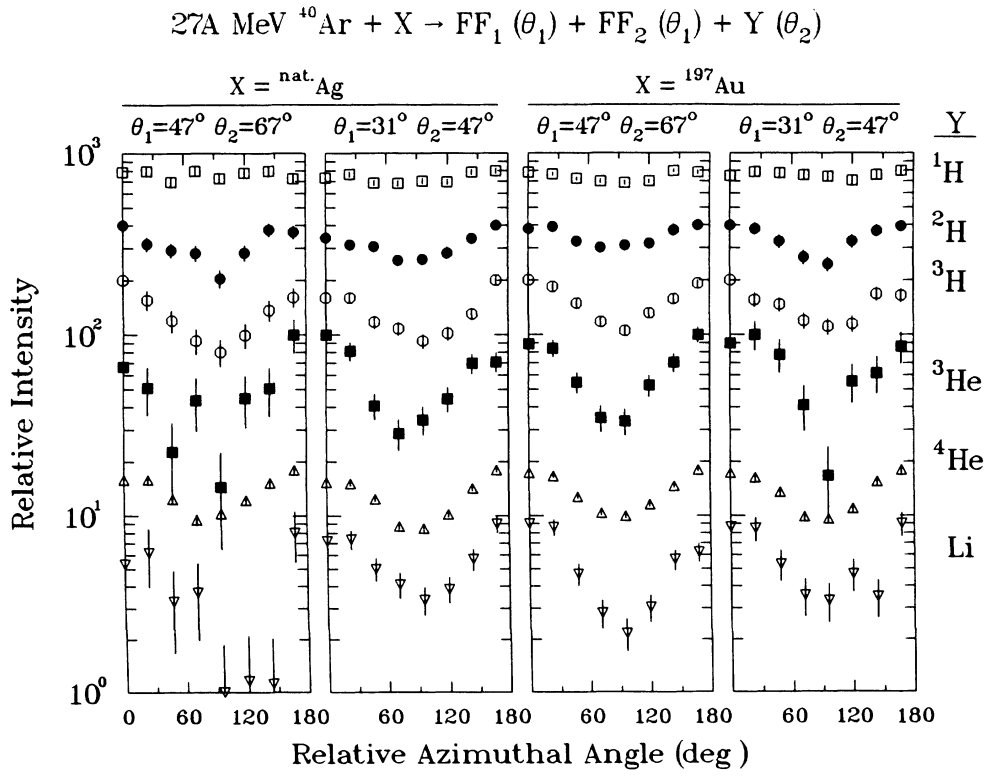

FIG. 10. Azimuthal angular correlations (θ and $\Delta\varphi$ in the laboratory frame) between fragment pairs ($Z > 3$) ($144° < \Delta\varphi < 216°$) and particles as indicated. Reactions with Ag or with Au are indicated.

includes effects of angular momentum along with three-body trajectory calculations for the two Li ejectiles and the recoil nucleus. Detector granularity and thresholds were included in the calculations. The ratio of intensities for $\Delta\varphi$ of 96° and 168° was used to assign an effective upper limit of $120\hbar$ for the triangular spin distribution. The shape near to $\Delta\varphi = 0°$ was used to explore the mean emitter lifetime; exponential decay was assumed with a single decay period. The best fit is provided by a meanlife of 5×10^{-22} s for the emitter. This result is of the same

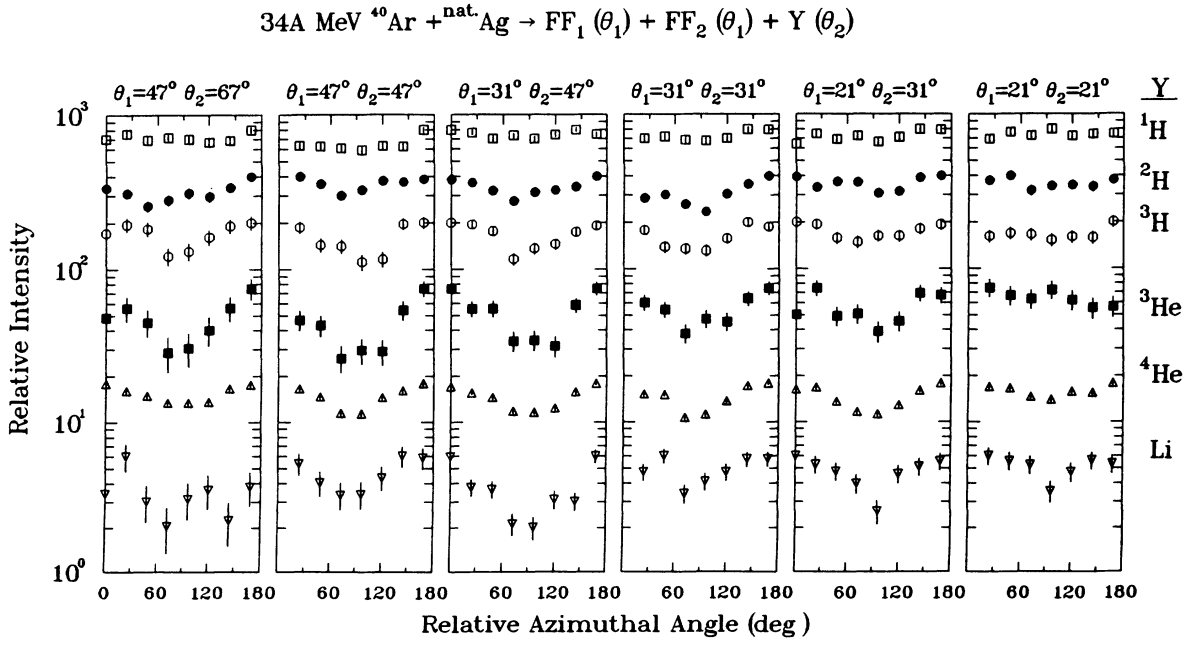

FIG. 11. Same as Fig. 10 but for 34 A MeV ^{40}Ar reactions and different angles as indicated.

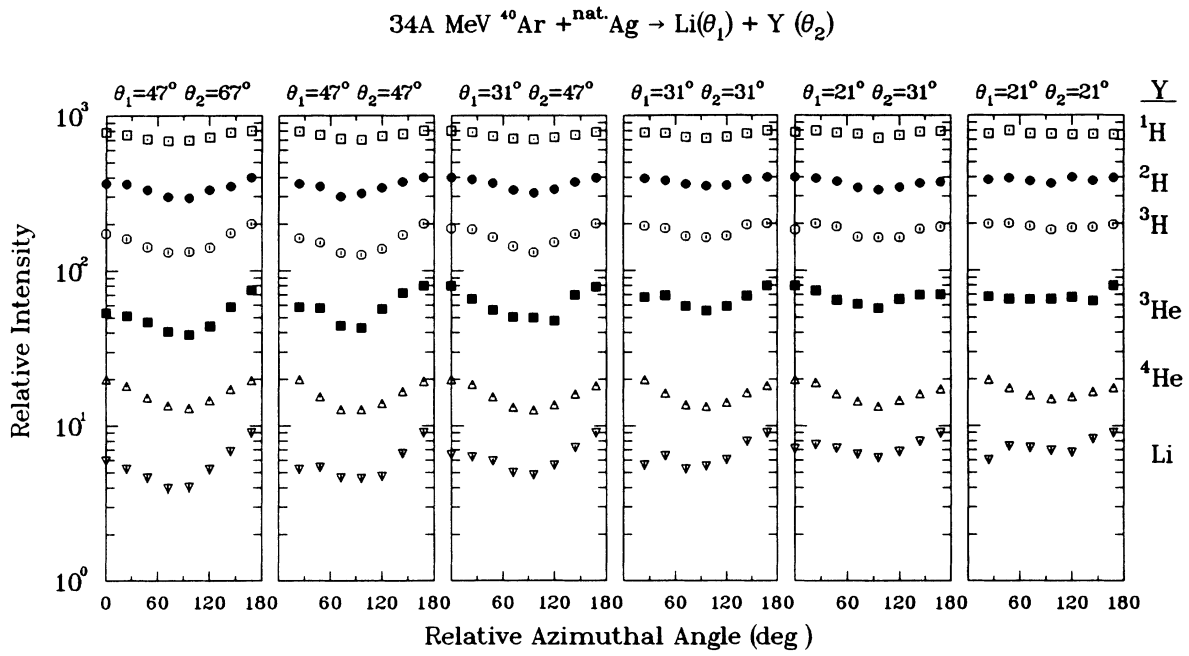

FIG. 12. Azimuthal angular correlations (θ and $\Delta\varphi$ in the laboratory frame) between Li fragments and other particles as indicated, 34 A MeV ^{40}Ar + ^{nat}Ag.

order as that found for evaporationlike light-particle pairs emitted in the reaction 680 MeV ^{40}Ar + Ag [28,30]. These mean times are each very short; indeed they suggest that it may be very difficult to distinguish evaporationlike emission from multifragmentation.

IV. SUMMARY AND CONCLUSIONS

This paper presents an overview of a number of properties of fragment emission in reactions of ^{40}Ar from 7 A to 34 A MeV. Fragments of $Z=3$ and $Z>3$ were recorded in four rings of CsI detectors centered at 21°, 31°, 47°, and 67°, each with 15 members to cover all azimuthal angles. For 7 A MeV ^{40}Ar+Ag and Au we confirm a large relative yield of fusion-fission fragments compared to a very small yield of intermediate-mass fragments and multifragment reactions. For 17 A MeV we also confirm the increasing importance of IMF and multifragment pro-

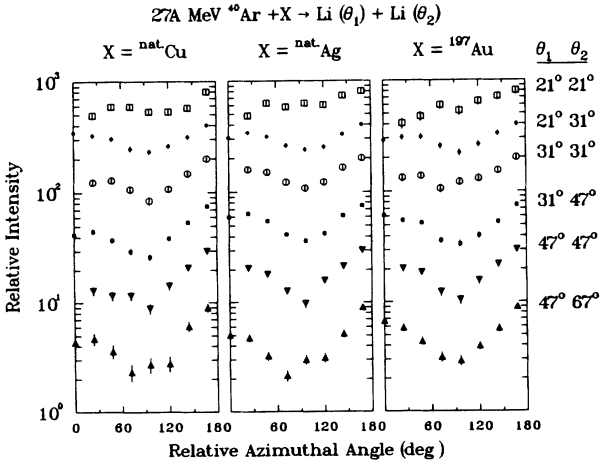

FIG. 13. Azimuthal angular correlations for Li-Li pairs for the angles indicated. Reactions of 27 A MeV ^{40}Ar with ^{nat}Cu, ^{nat}Ag, and ^{197}Au as shown.

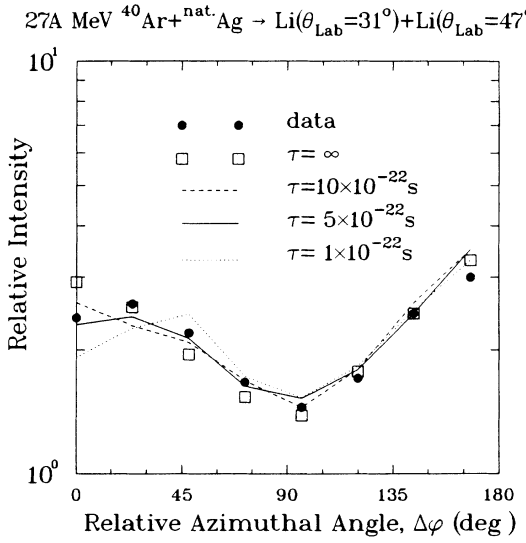

FIG. 14. Comparison of reaction simulations (based on Ref. [28]) for one data set for Li-Li pairs. For each simulation calcuation the emitter spins were taken to have a triangular spin distribution from 0 to 120$\hbar$. Emitter nuclei were assumed to decay exponentially with the mean lifetime indicated. Three-body trajectories were followed to account for the final-state interactions.

duction, but one still finds the continued dominance of classical fusion-fission. For 34 A MeV the folding-angle distributions become very similar for in-plane and out-of-plane fragment pairs, and no clear peak remains for classical fusion fission. One must conclude that the fragment mass distribution has become so wide that no clear border lines remain between reactions that give fission fragments, intermediate-mass fragments, or evaporation residues. A variety of fragment triggers are associated with large average multiplicities $\langle M_{\mathrm{H,He}} \rangle$ and similar H-He multiplicity distributions. However, the trigger requirement of three fragments ($Z > 3$) generates somewhat smaller H-He multiplicities than the two-fragment ($Z > 3$) trigger. This suggests that H-He multiplicity does not monotonically increase with collision centrality. Instead it implies that there is a large central collision group of reactions of similar violence and similar energy dissipation. All of these reactions seem to lead to great energy thermalization as evidenced by a strong component of nearly isotropic α-particle emission. Azimuthal angular correlations are reported for particles with respect to either two fission fragments ($Z > 3$) or with respect to single Li fragments. For both of these triggers the anisotropic disfavoring for $\Delta\varphi = 90°$ is approximately equivalent, indicating nearly equal strength of correlation with the reaction plane. The Li-Li correlations exhibit a distinct asymmetric preference for opposite side ($\Delta\varphi \approx 180°$) emission. The anisotropies and asymmetries of these two-body correlations give useful observables for testing reaction models for the dynamics of these complex heavy-ion reactions. For one case we show that these large-angle correlations can be accounted for by an emitter with spins of $(0-120)\hbar$ and mean delay time of 5×10^{-22} s between two Li ejectiles.

ACKNOWLEDGMENTS

Financial support has been provided by the United States Department of Energy and the Centre National de la Recherche Scientifique of France. Time and support from the Cornell National Supercomputer Facility is also appreciated. T.E. is also grateful to the Société Lyonnaise de Banque for partial support. We thank R. A. Lacey for many helpful ideas and discussions.

[1] For a summary see V. Viola, Nucl. Phys. **A502**, 531 (1989), and references therein.

[2] R. Vandenbosch and J. R. Huizenga, *Nuclear Fission* (Academic, New York, 1973).

[3] R. Freifelder, M. Prakash, and J. M. Alexander, Phys. Rep. **133**, 315 (1986).

[4] L. C. Vaz, J. M. Alexander, and N. Carjan, Z. Phys. A **324**, 331 (1986); J. M. Alexander, Ann. Phys. Fr. **12**, 603 (1987).

[5] N. N. Ajitanand, G. La Rana, R. Lacey, D. J. Moses, L. C. Vaz, G. F. Peaslee, D. M. de Castro Rizzo, M. Kaplan, and J. M. Alexander, Phys. Rev. C **34**, 877 (1986).

[6] S. Leray, G. Nebbia, C. Gregoire, G. La Rana, P. Lhenoret, C. Mazue, C. Ngô, M. Ribrag, E. Tomasi, S. Chiodelli, J. L. Charvet, and C. Lebrun, Nucl. Phys. **A425**, 345 (1984).

[7] M. F. Rivet, B. Borderie, H. Gauvin, D. Gardès, C. Cabot, F. Hanappe, and J. Peter, Phys. Rev. C **34**, 1282 (1986).

[8] G. Bizard, R. Brou, H. Doubre, A. Drouet, F. Guilbault, F. Hanappe, J. M. Haasse, J. L. Laville, C. LeBrun, A. Oubahadou, J. P. Patry, J. Peter, G. Ployart, J. C. Steckmeyer, and B. Tamain, Nucl. Phys. **A456**, 173 (1986).

[9] Y. Patin, S. LeRay, E. Tomasi, O. Granier, C. Cerruti, J. L. Charvet, S. Chiodelli, A. Demeyer, D. Guinet, C. Humeau, P. Lhenoret, J. P. Lochard, R. Lucas, C. Mazur, M. Morjean, C. Ngô, A. Peghaire, M. Ribrag, L. Sinopoli, T. Suomijarvi, J. Uzureau, and L. Vagneron, Nucl. Phys. **A457**, 146 (1986).

[10] H. Schulte, B. Jäckel, R. A. Esterlund, M. Knaack, W. Westmeir, A. Rox, and P. Patzelt, Phys. Lett. B **232**, 37 (1989).

[11] D. Jacquet, G. F. Peaslee, J. M. Alexander, B. Borderie, E. Duek, J. Galin, D. Gardes, C. Gregoire, D. Guerreau, H. Fuchs, M. Lefort, M. F. Rivet, and X. Tarrago, Nucl. Phys. **A509**, 195 (1990).

[12] D. Jouan, B. Borderie, M. F. Rivet, C. Cabot, H. Fuchs, H. Gauvin, F. Hanappe, D. Gardes, M. Montoya, B. Remaud, and F. Sebille, Z. Phys. A **340**, 63 (1991).

[13] D. Drain, A. Giorni, D. Hilscher, C. Ristori, J. Alarja, G. Barbier, R. Bertholet, R. Billerey, B. Chambon, B. Cheynis, J. Crancon, A. Dauchy, P. Désequelles, A. Fontenille, L. Guyon, D. Heuer, A. Lleres, M. Maurel, E. Monnand, C. Morand, H. Nifenecker, C. Pastor, J. Pouxe, H. Rossner, J. Saint-Martin, F. Schussler, P. Stassi, M. Tournier, and J. B. Viano, Nucl. Instrum. Methods A **281**, 528 (1989).

[14] R. T. de Souza, N. Cartin, Y. D. Kim, J. Ottarson, L. Phair, D. R. Bowman, C. K. Gelbke, W. G. Gong, W. G. Lynch, R. A. Pelak, T. Petrson, G. Poggi, M. B. Tsang, and H. M. Xu, Nucl. Instrum. Methods A **295**, 109 (1990).

[15] A. Chbihi, L. G. Sobotka, Z. Majka, D. G. Sarantites, D. W. Stracener, V. Abenante, T. M. Semkow, N. G. Nicolis, D. C. Hensley, J. R. Beene, and M. L. Halbert, Phys. Rev. C **43**, 652 (1991).

[16] D. A. Cebra, S. Howden, J. Karn, D. Kataria, M. Maier, A. Nadasen, C. A. Ogilvie, N. Stone, D. Swan, A. Vander Molen, LW. K. Wilson, J. S. Winfield, J. Yurkon, G. D. Westfall, and E. Norbeck, Nucl. Instrum. Methods A **300**, 518 (1991).

[17] T. Ethvignot, A. Elmaani, N. N. Ajitanand, J. M. Alexander, E. Bauge, P. Bier, L. Kowalski, M. T. Magda, P. Désesquelles, H. Elhage, A. Giorni, D. Heuer, S. Kox, A. Lleres, F. Merchez, C. Morand, D. Rebreyend, P. Stassi, J. B. Viano, S. Benrachi, B. Chambon, B. Cheynis, D. Drain, and C. Pastor, Phys. Rev. C **43**, R2035 (1991).

[18] M. T. Magda, T. Ethvignot, A. Elmaani, J. M. Alexander, P. Désesquelles, H. Elhage, A. Giorni, D. Heuer, S. Kox, A. Lleres, F. Merchez, C. Morand, D. Rebreyend, P. Stassi, J. B. Viano, F. Benrachi, B. Chambon, B. Cheynis, D. Drain, and C. Pastor, Phys. Rev. C **45**, 1209 (1992).

[19] T. Ethvignot, N. N. Ajitanand, J. M. Alexander, A. Elmanni, P. Désesquelles, H. Elhage, A. Giorni, D. Heuer, S. Kox, A. Lleres, F. Merchez, C. Morand, D. Rebreyend, P. Stassi, J. B. Viano, F. Benrachi, B. Chambon, B. Cheynis, D. Drain, and C. Pastor (unpublished); T. Ethvignot, Thèse de l'Université Joseph Fourier-Grenoble I, 1992; Institut des Sciences Nucleaire Report 92-31.

[20] J. Boger, S. Kox, G. Auger, J. M. Alexander, A. Naryanan, M. A. McMahan, D. J. Moses, M. Kaplan, and G. P. Gilfoyle, Phys. Rev. C **41**, R801 (1990).

[21] M. Conjeaud, S. Harar, M. Mostefai, E. C. Pollaco, C. Volant, Y. Cassagnou, R. Dayras, R. Legrain, H. Oeschler, and F. Saint-Laurent, Phys. Lett. **159B**, 244 (1985).

[22] E. Duek, L. Kowalski, M. Rajagopalan, J. M. Alexander, D. Logan, M. S. Zisman, and M. Kaplan, Z. Phys. A **307**, 221 (1982).

[23] R. Lacey, N. N. Ajitanand, J. M. Alexander, D. M. de Castro Rizzo, G. F. Peaslee, L. C. Vaz, M. Kaplan, M. Kildir, G. La Rana, D. J. Moses, W. E. Parker, D. Logan, M. S. Zisman, P. DeYoung, and L. Kowalski, Phys. Rev. C **37**, 2540 (1988).

[24] M. T. Magda, A. Elmaani, J. M. Alexander, T. Ethvignot, C. J. Gelderloos, P. Désesquelles, H. Elhage, A. Giorni, D. Heuer, S. Kox, A. Lleres, F. Merchez, C. Morand, D. Rebreyend, P. Stassi, J. B. Viano, F. Benrachi, B. Chambon, B. Cheynis, D. Drain, and C. Pastor (unpublished).

[25] W. K. Wilson, W. Benenson, D. A. Cebra, J. Clayton, S. Howden, J. Karn, T. Li, C. A. Ogilvie, A. Vander Molen, G. D. Westfall, J. S. Winfield, B. Young, and A. Nadasen, Phys. Rev. C **41**, R1881 (1990).

[26] M. B. Tsang, Y. D. Kim, N. Carlin, Z. Chen, C. K. Gelbke, W. G. Gong, W. G. Lynch, T. Murakami, T. Nayak, R. M. Ronningen, H. M. Xu, F. Zhu, L. Sobotka, D. W. Stracener, D. G. Sarantites, Z. Majka, and V. Abenante, Phys. Rev. C **42**, R15 (1990).

[27] G. D. Westfall, W. K. Wilson, C. A. Ogilvie, D. Krofcheck, A. M. Vander Molen, D. A. Cebra, J. S. Winfield, R. Lacey, T. Li, J. Yee, M. Cronquivst, and A. Nadasen, in *Collective Flow in Central and Peripheral Collisions of Intermediate Energy Heavy Ions,* Proceedings of the Seventh Winter Workshop on Nuclear Dynamics, edited by W. Bauer and J. Kapusta (World Scientific, Singapore, 1991), pp. 178–184.

[28] A. Elmaani, N. Ajitanand, T. Ethvignot, and J. M. Alexander, Nucl. Instrum. Methods A **313**, 401 (1992); A. Elmaani, Ph.D. thesis, State University of New York at Stony Brook, 1991.

[29] Y. D. Kim, R. T. de Souza, D. R. Bowman, N. Carlin, C. K. Gelbke, W. G. Gong, W. G. Lynch, L. Phair, M. B. Tsang, and F. Zhu, Phys. Rev. C **45**, 338 (1992).

[30] A. Elmaani, N. N. Ajitanand, J. M. Alexander, R. Lacey, S. Kox, E. Liatard, F. Merchez, T. Motobayashi, B. Noren, C. Perrin, D. Rebreyend, Tsan Ung Chan, G. Auger, and S. Groult, Phys. Rev. C **43**, R2474 (1991).

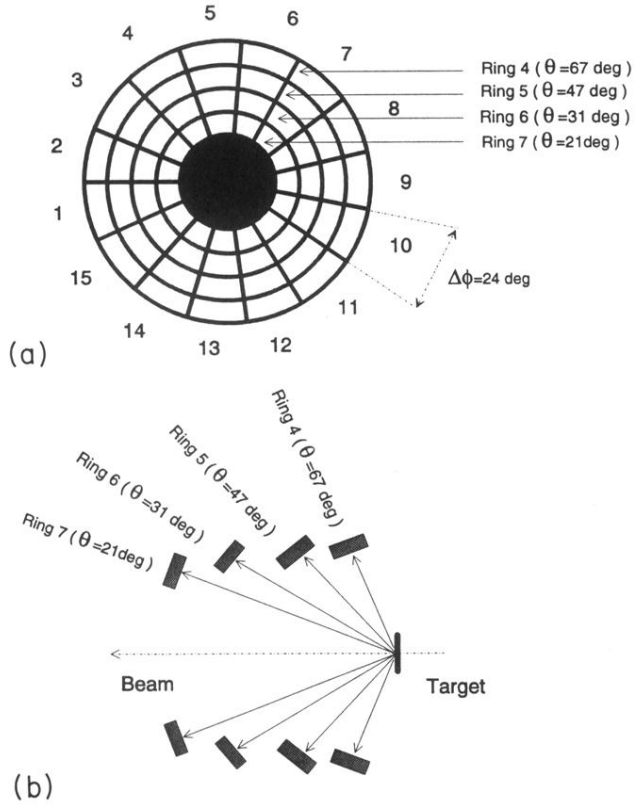

FIG. 1. Schematic diagram of the configuration of rings 4–7 of the AMPHORA multidetector (Ref. [13]). (a) View from the target in the beam direction; (b) side view.